International Refereed Journal of Engineering and Science (IRJES)
ISSN (Online) 2319-183X, (Print) 2319-1821
Volume 4, Issue 1 (January. 2015), PP. 83-87

Study of Core Shell Nanopectin

Rekha Sharma
Lecturer ,Department of Chemistry ,
Raj Rishi Govt. Atuonomus College ,
Alwar , Rajasthan , 301001

Abstract
Recent years have witnessed considerable efforts in the development of nanotechnology for drug delivery as it offers a suitable means of delivering both low molecular weight drugs and macromolecules either by localized or targeted delivery (Panyam & Labhasetwar, 2012). Nanoparticle drug delivery enhances the delivery or uptake by target cells and reduces the toxicity of the free drug to non-target organs, thereby increasing the therapeutic index (Singh et al., 2009). Cytotoxicity of nanoparticles or their biodegradation products remains a major concern and improving biocompatibility is clearly a major concern for future research (Dhanya et al., 2012). The use of natural polymers makes it possible to obtain materials with many interesting properties, such as low toxicity, biocompatibility and biodegradability, thus allowing their use as carriers (Müller et al., 2011). in this paper study of Core Shell Nanopectin

Keywords :- Preparation of nanoparticles , Preparation of nanoparticles , nanopectin UV- Visible spectroscopy , FT-IR spectroscopy & Conclusion

Preparation of nanoparticles
Zein Nanoparticles and Core shell Nanopectin encapsulating the model drug quercetin (a flavonoid) was prepared as described in Section. Characterization of nanoparticles

Preparation of nanoparticles.
Morphological characterization of the nanoparticles was performed using a scanning electron microscope (Figs. 1 and 2). The image reveals smooth zein nanospheres with an average size of 100 nm. The size of the nanoparticles ranged between 54-300nm. The size ranged from 54 to 178 nm for quercetin-encapsulated zein–pectin nanoparticles. The average size was 93nm. The difference in the size of the nanoparticles after the addition of the pectin solution may be due to their interaction with zein.

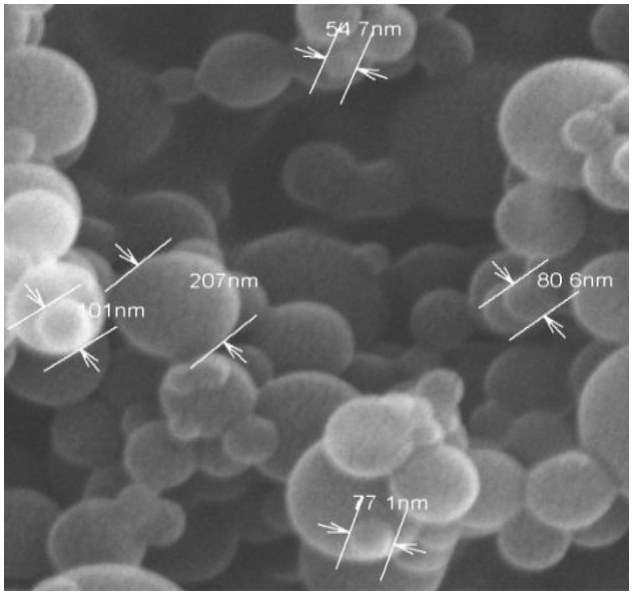

Figure 1: SEM image of nanozein

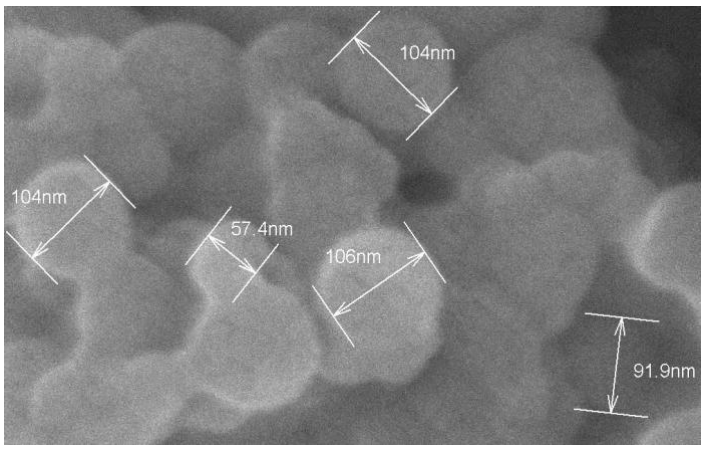

Figure 2: SEM image of quercetin encapsulated core-shell nanopectin UV- Visible spectroscopy

Overlay spectrum (Fig 3) shows UV-Vis spectra of the zein, quercetin, nanozein, drug loaded zein-pectin nanoparticle (80% ethanol as solvent), pectin and drug loaded zein-pectin nanoparticle (water as solvent). From the UV- Visible spectrum it can be observed that λ max of pure pectin matches with the λ max of drug loaded core shell – nanopectin (water as solvent for both) which confirms the presence of pectin in the drug loaded zein-pectin nanoparticle. λ max's of all other components were not visible since those are insoluble in water. When 80% ethanol was taken as solvent, λ max's of pure zein and quercetin was also seen in drug loaded nanozein in which zein and quercetin are incorporated and in drug loaded zein-pectin nanoparticle in which pectin, zein and quercetin was incorporated. From these data it can be assumed that core- shell nanopectin is formed and drug has been incorporated in the nanoparticle.

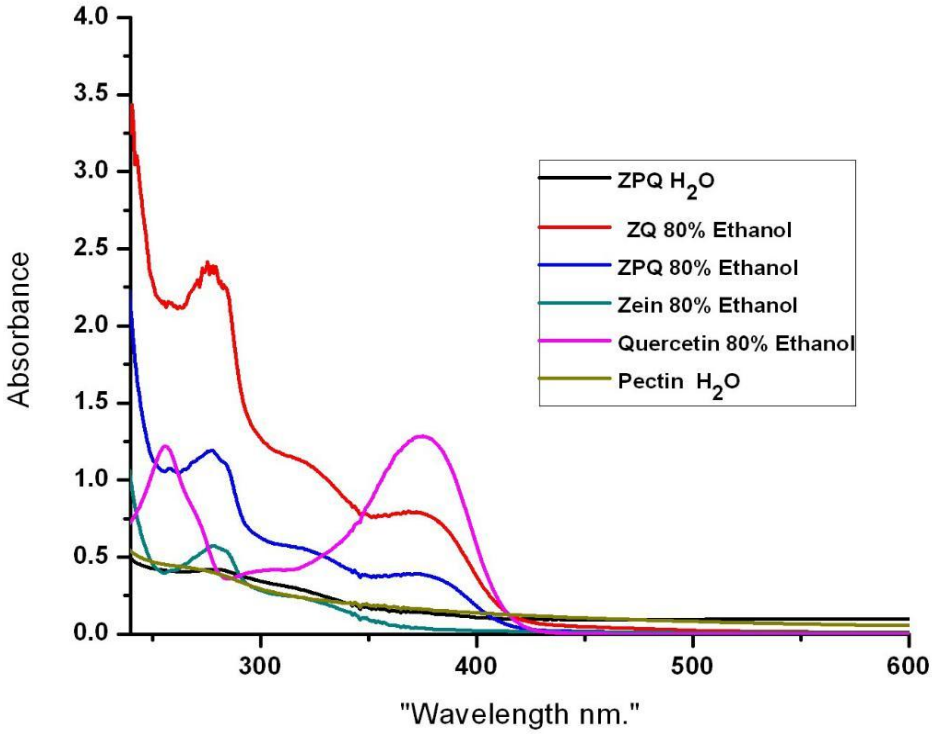

Figure 3: UV- Visible multispectra of zein, quercetin, nanozein, core – shell nanoparticle (80% ehanol as solvent), pectin and core – shell nanoparticle (water as solvent)

FT-IR spectroscopy

The comparison of FT-IR spectra of pectin from *Coccinia indica*, zein, quercetin (model drug), and drug loaded core shell nanopectin confirms the incorporation of all the components in core shell structure

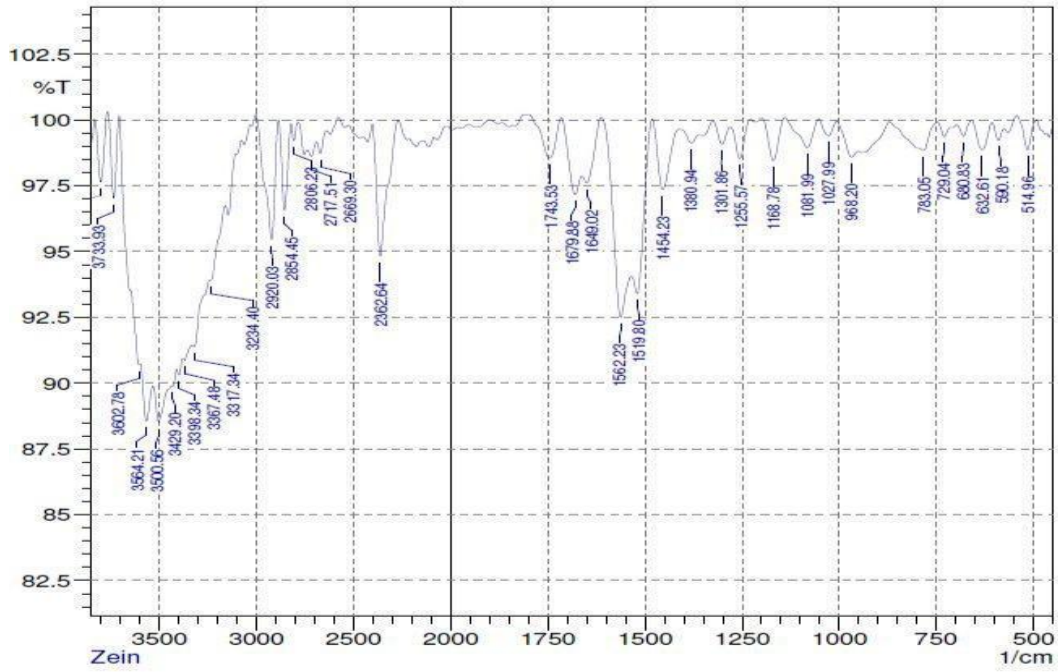

Figure 4: FT-IR Spectrum of Zein

FT – IR spectrum of zein (Fig. 4) exhibits an -OH peak at 3400 cm^{-1} and another peak at 1637 cm^{-1} indicates C-C multiple bond stretching. The peak at 1475 cm^{-}

is due to N-H bending vibrations of amine salts. Less intense peaks for -OH bending and stretching vibrations of 1^0, 2^0 and 3^0 alcohol are observed at 1287.5 cm^{-1} to1175 cm^{-1}. Two bands at 1225 cm^{-1} and 1037.5 cm^{-1} are due to C- N vibrations of aliphatic and aromatic moieties.

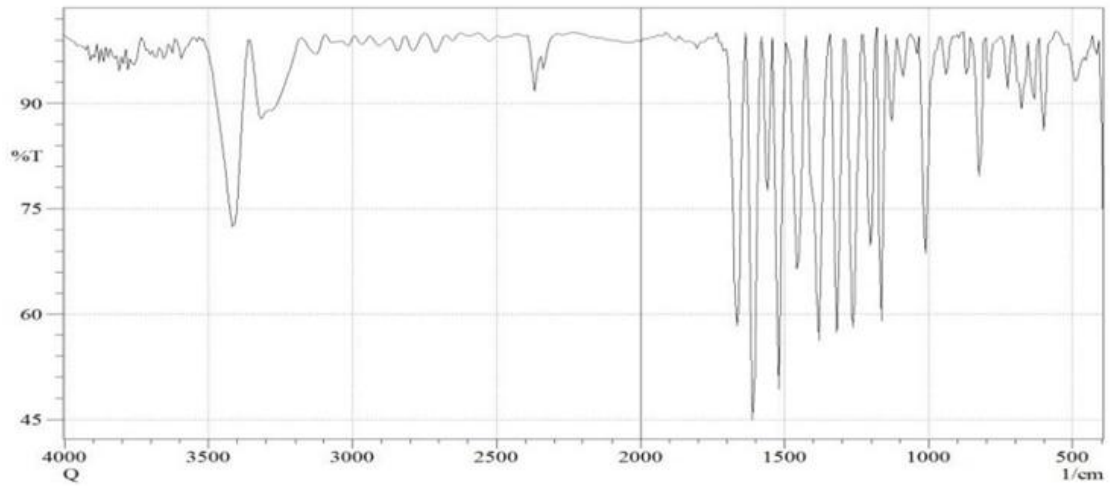

Figure 5 FT-IR Spectrum of Quercetin

FT-IR spectrum of quercetin (Fig. 5) shows intense peaks at 3411 cm^{-1} and 3311 cm^{-1} which may be due to the presence of –OH group. Another peak observed at 3125 cm^{-1} may be assigned to -OH stretching of the chelate compounds due to the polymeric association. A peak observed at 1687.5 cm^{-1} may be due to the ketone stretching. The peaks observed at 1512 cm^{-1} and 1450 cm^{-1} indicates the presence of aromatic C-C multiple bond stretching. The peak observed at 1300 cm^{-1} is due to OH bending and C-O stretching vibrations of phenols.

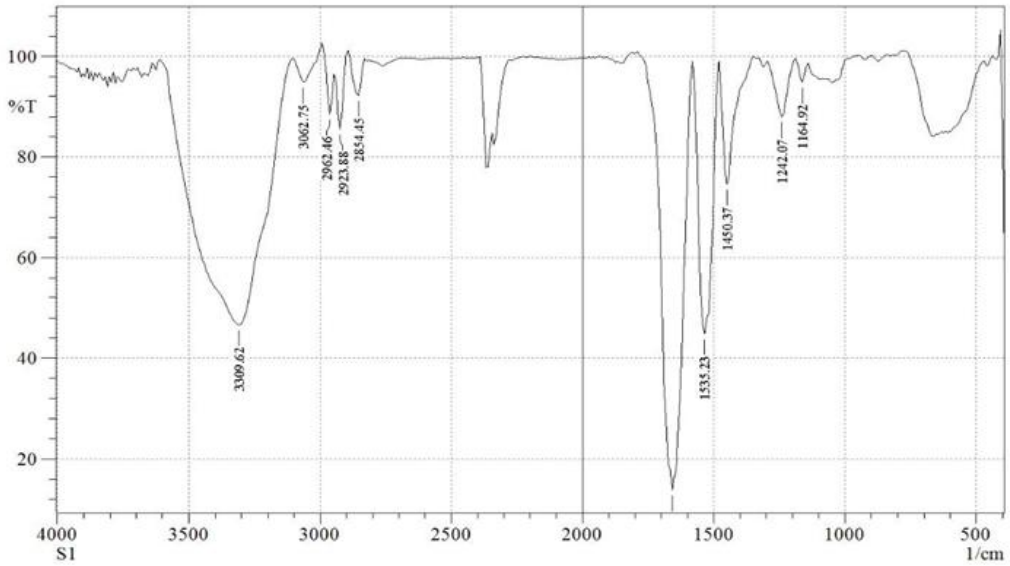

Figure 6: FT-IR Spectrum of Core –shell nanopectin

The FT-IR spectrum of drug-loaded zein-pectin nanoparticles (Fig. 6) shows very prominent peaks at 3300, 1650, 1540 and 1450 cm-1. The peak at 3300 cm-1, which is assigned to –OH, is found to be shifted from the range of 3400 cm-1 in pectin, zein and quercetin, which may be due to the interactions of –OH groups between them. The peak at 1650 cm-1 may be due to the C-C multiple bond stretching in the tetra substituted alkene being shifted to a higher wave number. The peaks at 1540 and 1510 cm-1 can be assigned to -NH bending vibrations, which can also be observed in pectin and zein. Another peak at 1450 cm-1 may be due to the stretching of C-C multiple bonds of aromatic compounds, which show the presence of quercetin in the zein-pectin nanoparticle. A new band at 1748 cm-1 assigned to C=O from –COOH confirms the presence of pectin in the developed nanoparticles. Another band observed at 1300 cm-1, which can be assigned to the OH bending and C-O stretching vibrations of phenols, confirms the presence of the model drug quercetin.
By correlating the results of UV-visible and FT-IR spectroscopy, it can be assumed that a core-shell nanopectin was formed and the drug was incorporated into the nanoparticle.

Conclusion:-

This preliminary study envisages the use of natural polymers and herbal extract for the formulation of a nano antidiabetic drug. The investigation highlighted MPENs that demonstrated good drug entrapment ability, thermal stability, and sustained drug release properties. The developed nanoparticles can be used as a drug delivery system for sustained drug release.

REFERENCES

[1]. Ashok Kumar, B. S., Lakshman, K., Jayaveera, K. N., Sheshadri Shekar, D., Narayan Swamy, V. B., Khan, S., & Velumurga, C. (2011). In vitro α-amylase inhibition and antioxidant activities of methanolic extract of Amaranthus caudatus Linn. *Oman Medical Journal*, *26*(3), 166–170.
[2]. Babu, V., Gangadevi, T., & Subramoniam, A. (2003). Antidiabetic Activity of Ethanol extract of Cassia kleinii Leaf in Streptozotocin-Induced Diabetic Rats and Isolation of an Active Fraction and Toxicity Evaluation of the Extract. *Indian Journal of Pharmacology*, *35*, 290–296.
[3]. Chittasupho, C., Jaturanpinyo, M., & Mangmool, S. (2013). Pectin nanoparticle enhances cytotoxicity of methotrexate against hepG2 cells. *Drug Delivery*, *20*(1), 1–9.
[4]. Cho, K., Wang, X., Nie, S., Chen, Z., Shin, D. M. (2008). Therapeutic Nanoparticles for Drug Delivery in Cancer. *Clinical Cancer Research*, *14*(5), 1310–1316
[5]. Dobies, M., Kuśmia, S., & Jurga, S. (2005). ^{1}H NMR and rheological studies of the calcium induced gelation process in aqueous low methoxyl pectin solutions. *Acta Physica Polonica A*, *108* (1), 33–46.
[6]. E. W. Yemm & A. J. Willis. (1954). The Estimation of Carbohydrates in Plant Extracts by Anthrone. *Biochemistry*, *57*, 508–514.
[7]. Fishman, M. L., Chau, H. K., Hoagland, P., & Ayyad, K. (2000). Characterization of pectin, flash-extracted from orange albedo by microwave heating, under pressure. *Carbohydrate Research*, *323*, 126–138.
[8]. Girish, K. S., Mohanakumari, H. P., Nagaraju, S., Vishwanath, B. S., & Kemparaju, K. (2004). Hyaluronidase and protease activities from Indian snake venoms : neutralization by Mimosa pudica root extract. *Fitoterapia*. *75*, 378–380.
[9]. Harizal, S. N., Mansor, S. M., Hasnan, J., Tharakan, J. K. J., & Abdullah, J. (2010). Acute toxicity study of the standardized methanolic extract of Mitragyna speciosa Korth in Rodent. *Journal of Ethnopharmacology*, *131*(2), 404–409.
[10]. Hashim, A., Khan, M. S., Khan, M. S., Baig, M. H., & Ahmad, S. (2013). Antioxidant and α; ylase inhibitory property of phyllanthus virgatus L.: An in vitro and molecular interaction study. *BioMed Research International*. *2013*, 12 pages.
[11]. Nozzolillo, C. (1973). A survey of anthocyanin pigments in seedling legumes. *Canadian Journal of Botany,51,* 911-915.

[12]. OECD. (2001). Acute Oral Toxicity – Fixed Dose Procedure (chptr). *OECD Guideline for Testing of Chemicals*, (December), 1–14.
[13]. Priyadarsini, S. S., Vadivu, R., & Jayshree, N. (2010). In vitro and In vivo antidiabetic activity of the leaves of Ravenala madagascariensis Sonn ., on alloxan induced diabetic rats. *Journal of Pharmaceutical Science and Technology*, *2*(9), 312–317.
[14]. Tyagi, S., Singh, G., Sharma, A., & Aggarwal, G. (2010). Phytochemicals as Candidate Therapeutics : An Overview. *International Journal of Pharmaceutical Sciences Review and Research*, *3*(1), 53–55.
[15]. Viswanathan R, Sekar, V., Velpandian, V., Sivasaravanan, K., & Ayyasamy, S. (2013). Anti-diabetic activity of Thottal vadi choornam (Mimosa pudica) in Alloxan Induced Diabetic Rats. *International Journal of Natural Product Science*, *3*(5), 13–20.
[16]. Wang, S., & Dormidontova, E. E. (2010). Nanoparticle design optimization for enhanced targeting: Monte carlo simulations. *Biomacromolecules*, *11*(7), 1785– 1795.
[17]. Xie, G., Sun, J., Zhong, G., Liu, C., & Wei, J. (2010). Hydroxyapatite nanoparticles as a controlled-release carrier of BMP-2: Absorption and release kinetics in vitro. *Journal of Materials Science: Materials in Medicine*, *21*(6), 1875–1880
[18]. Yerragunta, V., Kumaraswamy, T., Suman, D., Anusha, V., Patil, P., & Samhitha, T. (2013). A review on Chalcones and its importance. *PharmaTutor Magazine*, *1*(2), 54–59.